ELSEVIER

Journal of Alloys and Compounds 338 (2002) 87–92

Journal of ALLOYS AND COMPOUNDS

www.elsevier.com/locate/jallcom

Synthesis, characterization and bonding of $Ba_3Li_4Sn_8$

Svilen Bobev, Slavi C. Sevov*

Department of Chemistry and Biochemistry, University of Notre Dame, Notre Dame, IN 46556, USA

Received 18 October 2001; accepted 26 November 2001

Abstract

The ternary compound $Ba_3Li_4Sn_8$ was obtained by slow cooling of a stoichiometric mixture of the elements that was heated at 800 °C for 2 days. Its structure (monoclinic, *C2/m*, $Z=2$, $a=18.549(1)$, $b=6.685(1)$, $c=6.792(1)$ Å, $V=833.2(2)$ Å^3, $R_1/wR_2 = 4.03/11.33\%$) contains one-dimensional chains of $^1_\infty[Sn_8]^{10-}$ made of edge-sharing cyclodecane-like units in their 'all-chair' conformations. The cations screen the chains from each other and provide the extra electrons needed for bonding in the chains. The structure and the electron count can be rationalized in terms of the Zintl concept as $(Ba^{2+})_3(Li^+)_4[(2b\text{-}Sn^{2-})_2(3b\text{-}Sn^{1-})_6]$, i.e. the compound is an electronically balanced, Zintl phase. Nevertheless, $Ba_3Li_4Sn_8$ exhibits temperature-independent paramagnetism that is, most likely, of van Vleck type as a result of the very small band gap of about 0.3 eV.

Keywords: Intermetallic; Zintl phases; X-ray diffraction; Electronic band structure

1. Introduction

The discovery of Tt_9^{4-} in neat solids (Tt=Tetrel, element of group 14) stimulated the search for Zintl phases with other isolated clusters, either new or similar to those known as crystallized from solutions [1–6]. Our thorough and systematic studies of the binary A–Tt systems (A= alkali metal) extended into the pseudo-binary systems with mixed alkali metals, especially combinations of very different sizes, and provided the first *arachno*-clusters of group 14, Sn_8^{6-} in $A_4Li_2Sn_8$ for A=K or Rb [7]. Similarly, germanium forms novel giant clusters, truncated tetrahedra of Ge_{12}^{12-}, when combined with a mixture of Li and Rb in $RbLi_7Ge_8$ [8]. It is important to emphasize that both novel species form only in Li-containing, mixed alkali-metal phases, and not in simple binaries. Besides the role of the sizes of the cations these phases are apparently stabilized also by the better covalency of lithium which caps the open faces of these clusters and stabilizes them as *closo*-species, $Li_2Sn_8^{4-}$ and $Li_4Ge_{12}^{8-}$ [7,8]. Also, mixed alkali metals provide compounds with isolated clusters of lead, Pb_4^{4-}-tetrahedra and Pb_9^{4-} of different shapes [9]. Following the studies of the pseudo-binary systems with mixed alkali metals we have taken one step further in complexity and have studied the systems alkali-metal (A)–alkaline-earth metal (AE)–tetrel (Tt). Found in these systems were truncated tetrahedra of Sn_{12}^{12-} in $[AE]Na_{10}Sn_{12}$ for AE=Ca or Sr [10], and similar to the lithium-stabilized *closo*-$Li_4Ge_{12}^{8-}$, they are stabilized by sodium as *closo*-$Na_4Sn_{12}^{8-}$ clusters. Using Ba instead of Ca or Sr led to the formation of the largest naked cluster of a main-group element, Sn_{56}^{44-} in $Ba_{16}Na_{204}Sn_{310}$ [11]. This cluster is made of four fused pentagonal dodecahedra of tin that are stuffed with four barium cations. Here we report the synthesis and structural characterization of another compound with mixed alkali and alkaline-earth cations, $Ba_3Li_4Sn_8$. It exhibits one-dimensional chains of $^1_\infty[Sn_8]^{10-}$ that are made of edge-sharing cyclodecane-like units in their 'all-chair' conformation, unprecedented structural motifs in the chemistry of the heavier carbon homologues.

2. Experimental section

2.1. Synthesis

All manipulations were performed in an Ar-filled glove box. The surfaces of Li (rod, Aldrich, 99.9%, sealed under

*Corresponding author. Tel.: +1-219-631-5891; fax: +1-219-631-6652.

E-mail address: ssevov@nd.edu (S.C. Sevov).

0925-8388/02/$ – see front matter
PII: S0925-8388(02)00219-0

Ar) and Ba (rod, Alfa, 99.2%, sealed under Ar) were cleaned off with a scalpel immediately before use, while Sn (rod, Alfa, 99.999%) was used as received. All reactions were carried out in sealed niobium tubes, which were in turn jacketed and sealed under vacuum in silica ampoules. More details on the techniques and the procedures are described elsewhere [12].

Initially, $Ba_3Li_4Sn_8$ was synthesized as the major product of a reaction designed to produce $BaLi_{10}Sn_{12}$, the barium–lithium analog of $[AE]Na_{10}Sn_{12}$ (AE = Ca, Sr) [10]. The reaction was carried out at 800 °C (m.p. of Ba is 725 °C; no phase diagram for Ba–Sn; the highest m.p. in Li–Sn is 780 °C) for 48 h and cooled down to room temperature with a rate of 5 °C/h. Other products from that reaction, as identified by powder X-ray diffraction (Enraf-Nonius Guinier camera with a vacuum chamber and Cu Kα radiation), were traces of $BaSn_3$ and LiSn as well as some unreacted Sn metal. After the stoichiometry of the compound was obtained from the structure determination, stoichiometric mixtures were treated at the same temperature regimes. A least-squares refinement of the measured 2θ values of the X-ray powder diffraction pattern of the compound relative to those of the internal standard (silicon) verified the lattice constants.

2.2. Structure determination

Numerous crystals of $Ba_3Li_4Sn_8$ were selected in the glove box and were sealed in 0.2 mm thin-walled glass capillaries. They were checked for singularity on an Enraf-Nonius CAD4 single-crystal diffractometer (graphite-monochromated Mo Kα radiation, $\lambda = 0.71073$ Å). One of these crystals (irregular, $0.16 \times 0.14 \times 0.08$ mm) was chosen and a unique quadrant of X-ray diffraction data was collected at room temperature with ω–2θ scans and up to 2θ of 60°. All 2013 reflections were corrected for absorption with the aid of the average of ψ-scans of four reflections at different θ angles ($R_{int} = 0.051$; $T_{min}/T_{max} = 0.154/0.316$). The observed extinction conditions and the intensity statistics suggested the centrosymmetric space group *C2/m*. Consequently, the structure was successfully solved and refined with the aid of the SHELXTL-V5.1 software package [13] in that space group. The direct methods provided three peaks with distances to each other appropriate for tin atoms, and two peaks with distances to the other three that were appropriate for barium atoms, and they were all so assigned. The following least-squares cycles and a difference Fourier synthesis revealed two peaks at special positions and with relatively low heights. These were assigned as lithiums, and the subsequent anisotropic refinement of all atoms converged at $R_1 = 4.17\%$; $wR_2 = 11.43\%$ for 1309 independent reflections and 43 parameters. Further details on the data collection and refinement parameters are summarized in Table 1, while positional and equivalent isotropic displacement parameters and important distances are listed in Tables 2 and 3, respectively.

Table 1
Selected data collection and refinement parameters for $Ba_3Li_4Sn_8$

Chemical formula	$Ba_3Li_4Sn_8$
Formula weight	1389.30
Space group, *Z*	*C2/m* (No. 12), 2
Unit cell parameters (Å)	$a = 18.549(1)$
	$b = 6.685(1)$
	$c = 6.792(1)$
	$\beta = 98.34(1)°$
	$V = 833.2(2)$ Å^3
Radiation, λ (Å)	Mo Kα, 0.71073
2θ limit	60°
μ (cm^{-1})	186.84
ρ_{calcd} (g/cm^3)	5.538
Data/restraints/parameters	1309/0/43
R indices ($I > 2\sigma_I$)[a]	$R_1 = 4.03\%$, $wR_2 = 11.33\%$
R indices (all data)	$R_1 = 4.17\%$, $wR_2 = 11.43\%$

[a] $R_1 = \Sigma||F_o| - |F_c||/\Sigma|F_o|$; $wR_2 = [\Sigma[w(F_o^2 - F_c^2)^2]/\Sigma[w(F_o^2)^2]]^{1/2}$. $w = 1/[\sigma^2 F_o^2 + (0.0673P)^2 + 29.333P]$, $P = (F_o^2 + 2F_c^2)/3$.

2.3. Magnetic measurements

The magnetizations of different samples of $Ba_3Li_4Sn_8$ were measured on a Quantum Design MPMS SQUID magnetometer at a field of 30 kG over the temperature range 10–280 K. Measurements at lower temperatures (down to 4 K) and lower magnetic fields of 50, 100 and 300 G were carried out as well. The samples were contained in special holders designed for air-sensitive compounds [12]. The raw data were corrected for the holder contribution and for ion-core diamagnetism. The corrected magnetic susceptibility is positive and temperature independent, and varies between 4.17×10^{-4} and 4.98×10^{-4} emu/mol (average of two measurements on two different samples). No superconductivity was observed at the low temperatures and magnetic fields.

2.4. Band calculations

Extended Hückel band calculations were carried out within the tight binding approximation with only the tin atoms included (H_{ii} and ζ_1 for Sn 5s: −16.16 eV and 2.12, for Sn 5p: −8.32 eV and 1.82) [14]. The density of states

Table 2
Atomic coordinates and equivalent isotropic displacement parameters (Å^2) for $Ba_3Li_4Sn_8$

Atom	Site	*x*	*y*	*z*	U_{eq}
Sn1	4*i*	0.12920(4)	0	0.4541(1)	0.0142(2)
Sn2	4*i*	0.48483(4)	0	0.2020(1)	0.0145(2)
Sn3	8*j*	0.85055(3)	0.73248(8)	0.19789(8)	0.0141(2)
Ba1	2*a*	0	0	0	0.0135(2)
Ba2	4*i*	0.32245(4)	0	0.6913(1)	0.0153(2)
Li1	4*h*	0	0.787(4)	1/2	0.029(5)
Li2	4*i*	0.209(1)	0	0.130(4)	0.022(4)

Table 3
Important bond distances (Å) and angles (°) in $Ba_3Li_4Sn_8$

Sn1–	2×	Sn3	2.9440(9)	Li1–	2×	Sn1	2.84(1)
	2×	Li1	2.84(1)		2×	Sn2	2.77(2)
		Li2	2.82(2)		2×	Sn3	3.221(3)
		Ba1	3.6211(9)			Li1	2.85(6)
	2×	Ba2	3.6342(6)		2×	Ba1	3.68(1)
		Ba2	3.711(1)	Li2–		Sn1	2.82(2)
Sn2–		Sn2	2.880(2)		2×	Sn3	2.94(2)
	2×	Sn3	2.9325(8)		2×	Sn3	3.03(2)
	2×	Li1	2.77(2)		2×	Ba2	3.630(9)
	2×	Ba1	3.6393(6)	Ba1–	2×	Sn1	3.6211(9)
		Ba2	3.543(1)		4×	Sn2	3.6393(6)
Sn3–		Sn1	2.9440(9)		2×	Sn3	3.7107(6)
		Sn2	2.9325(8)		4×	Li1	3.68(1)
		Sn3	3.108(1)	Ba2–	2×	Sn1	3.6342(6)
		Li1	3.221(3)			Sn1	3.711(1)
		Li2	2.94(2)			Sn2	3.543(1)
		Li2	3.03(2)		2×	Sn3	3.7422(9)
		Ba1	3.7107(6)		2×	Sn3	3.7977(9)
		Ba2	3.7422(9)		2×	Sn3	3.8421(8)
		Ba2	3.7977(9)		2×	Li2	3.630(9)
		Ba2	3.8421(8)				
Sn3–Sn1–Sn3			74.81(3)	Sn2–Sn3–Sn1			107.75(3)
Sn2–Sn2–Sn3			105.90(4)	Sn2–Sn3–Sn3			58.00(1)
Sn3–Sn2–Sn3			64.00(3)	Sn1–Sn3–Sn3			127.40(2)

and the crystal orbital overlap populations were calculated on the basis of 240 k-points over the irreducible wedge of the Brillouin zone.

3. Results and discussion

3.1. Structure description

The structure of $Ba_3Li_4Sn_8$ consists of isolated chains of tin that run along the *b* axis of the monoclinic cell (Fig. 1). The repeating monomeric unit of the chains is cyclodecane in its 'all-chair' conformation (Fig. 2). Each monomer shares two directly opposite edges with its two neighbors in the chain. Interestingly, there is another compound in the ternary (AE)–Li–Tt system with almost the same composition, $Ca_{3+x}Li_{4-x}Si_8$ [15], and its structure, although different from $Ba_3Li_4Sn_8$, contains also chains of the tetrel. The difference is that the chains of silicon are made of interconnected xylene-like rings rather than fused cyclodecanes. The cyclodecanes in $Ba_3Li_4Sn_8$ are made of three unique tin sites (Fig. 2), two of which, Sn2 and Sn3, are three-bonded, while the third, Sn1, is two-bonded. The Sn–Sn distances within the cyclodecane monomer are quite similar, 2.880(2)–2.9440(9) Å (Table 3). They are typical for single, localized Sn–Sn bonds such as those found in Sn_4^{4-} tetrahedra and $^1_\infty[Sn]^{2-}$ zigzag chains [16]. The edges that are shared with neighboring cyclodecanes are Sn2–Sn2 pairs. This brings the Sn3 atoms (the atoms next to the shared edges) of different cyclodecanes in relatively close proximity, 3.108 Å. Thus, a triangle of one Sn2 and two Sn3 atoms is formed when the Sn3–Sn3

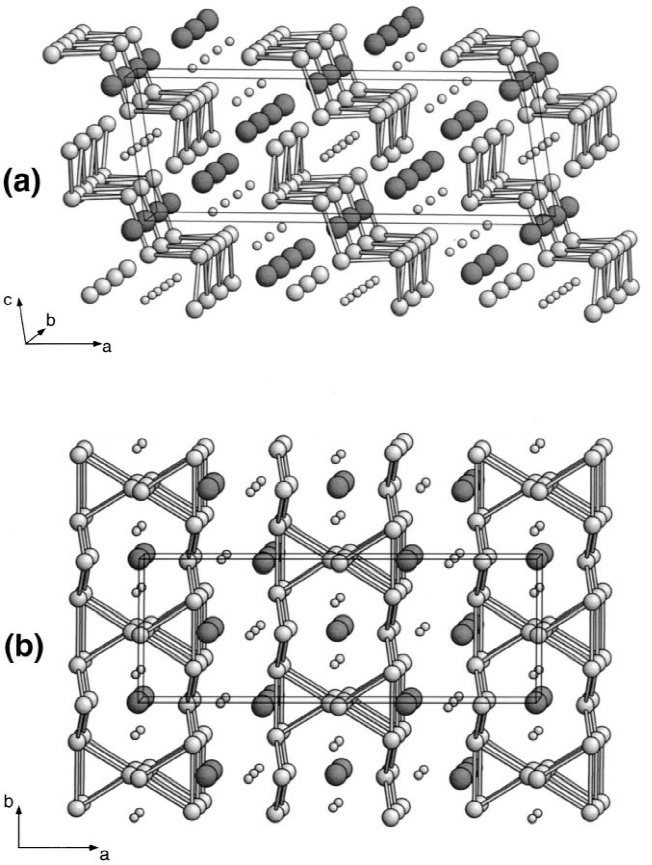

Fig. 1. General view of the *C*-centered monoclinic structure of $Ba_3Li_4Sn_8$ viewed: (a) along the *b* axis, and (b) along the *c* axis. The large and small isolated spheres are Ba and Li atoms, respectively. The unit cell is outlined.

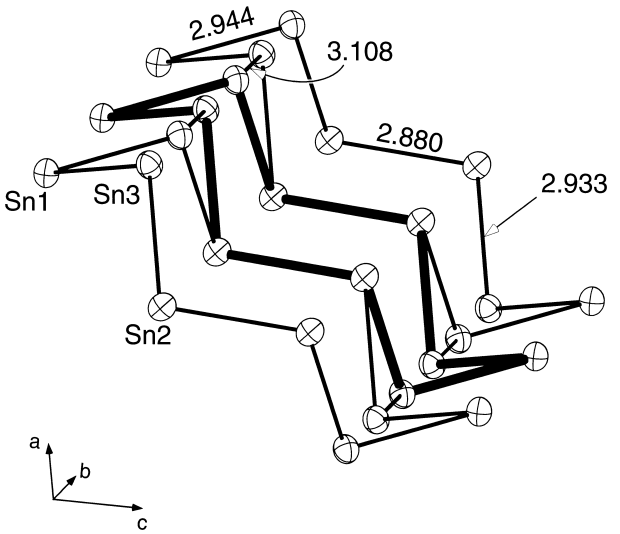

Fig. 2. An ORTEP drawing (80% probability thermal ellipsoids) of a three-monomer section of the $^1_\infty[Sn_8]^{10-}$ chain. The monomer is with the shape of a cyclodecane in its 'all-chair' conformation (outlined). Each cyclodecane shares two opposite edges with two neighbors.

contact of 3.108(1) Å is considered. This distance is somewhat longer but compares well with the distances in metallic β-Sn, 3.016 and 3.175 Å [16], in $BaSn_3$ with isolated triangular Sn_3^{2-} units, 3.058 Å [17], and in $Ca_{31}Sn_{20}$ with Sn_2^{6-} dimers and Sn_5^{12-} linear pentamers, 3.063–3.158 Å [18], and should be considered in the bonding picture. Longer distances in lithium-containing compounds have been discussed extensively elsewhere [19]. The elongation, usually in the order of 0.15 Å relative to Sn–Sn single-bond distance, is explained by the strong cation field effects and strong polarizing power of lithium [19].

The angles at the tin atoms deviate substantially from the ideal tetrahedral angle and are in a very wide range, all the way from 58.00(1) to 107.75(3)°. As might be expected, the sharpest angles are within the isosceles triangle of two Sn3 and one Sn2 atoms, 58.00(1) and 64.00(3)°. These are followed by the angle at the two-bonded Sn1, 74.81(3)°, for which a relatively small angle is normal due to the two lone pairs of electrons associated with it. The remaining angles are closer to tetrahedral. It should be pointed out that isolated triangular units of Sn_3^{2-} with two delocalized π electrons that are isoelectronic with the aromatic cyclopropenium cation $C_3H_3^+$ exist in $BaSn_3$ [18].

3.2. Electronic structure

The electron needs for bonding in the chains can be discerned based on the octet rule. Thus, a three-bonded pyramidal atom such as Sn2 and Sn3 carries a lone pair of electrons and must provide an electron for each bond, or a total of five electrons per atom. A two-bonded atom such as Sn1 carries two lone pairs of electrons in addition to the two electrons of the two bonds, or a total of six electrons. This means that the formal oxidation state for Sn2 and Sn3 is 1− while for Sn1 it is 2−. Thus, the need of additional electrons for the bonding of the repeating unit of two Sn1, two Sn2, and four Sn3 atoms becomes $2\times(2-)+2\times(1-)+4\times(1-)=10-$. Exactly that many electrons are available from the three Ba and four Li atoms in the formula of the compound, $Ba_3Li_4Sn_8$, and therefore the compound should be electronically-balanced, or a Zintl phase.

This simple counting scheme assumes, of course, complete electron transfer from the alkali and alkaline-earth metals to the post-transition element. However, it does not provide insight into the electron distribution among the different Sn–Sn bonds or the strength of the different interactions. Furthermore, actual negative charges rarely correspond to the assigned formal oxidation states. In order to study the bonding of $Ba_3Li_4Sn_8$ in more detail and to eventually relate its structure to the observed temperature-independent paramagnetism, extended Hückel band calculations were carried out for the Sn sublattice. The total density of states (DOS) is shown in Fig. 3 together with the projected partial DOS of Sn3. The total of 42 electrons for the repeating unit Sn_8^{10-} fill the bands below the Fermi level at −5.12 eV. Thus, the valence band is completely filled and is separated by a very narrow gap of less than 0.3 eV from the conduction band. This suggests that the observed temperature-independent paramagnetism of $Ba_3Li_4Sn_8$ is either of van Vleck type, i.e. paramagnetism due to mixing of the ground state (filled valence band) with thermally-empty, yet low-lying, excited paramagnetic states (conduction band), or that simply the conduction and valence bands overlap. The latter is quite possible because, as it is well known, extended-Hückel calculations are only an approximation and often overestimate the band gaps. Furthermore, we should keep in mind that the calculations did not include the cation–anion interactions, which will further perturb the overall widths and positions of the valence and conduction bands, and may very well cause overlap between them. These interactions, especially with lithium may have significant covalent character as already pointed out.

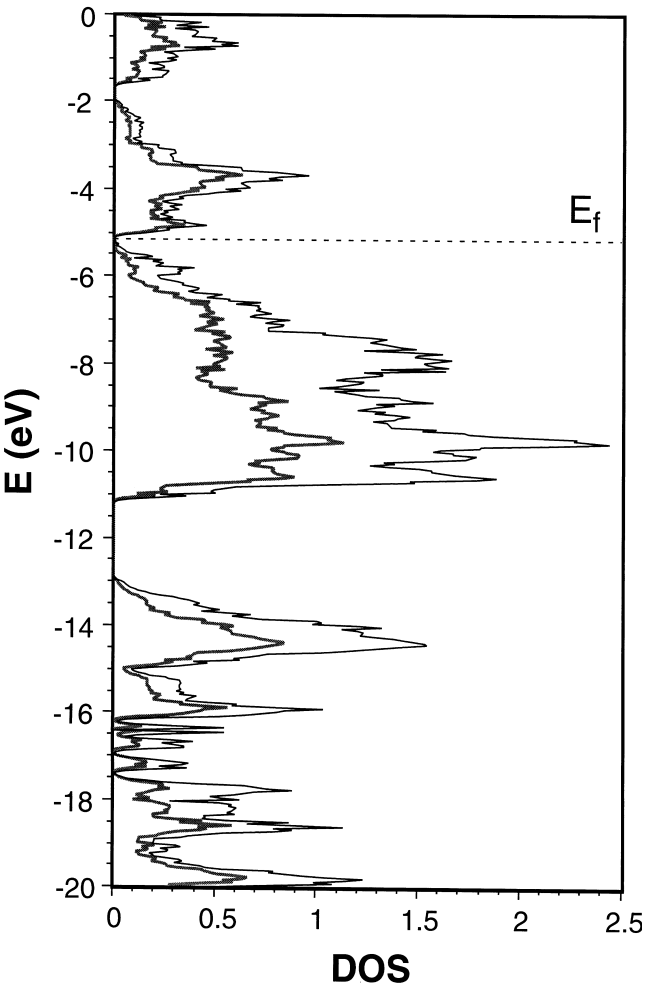

Fig. 3. Shown are the total DOS (black line), the projected partial DOS of Sn3 (gray line), and the Fermi level (broken line) for $Ba_3Li_4Sn_8$. A very small band gap of less than 0.3 eV separates the valence and conduction bands.

Closer look at the DOS (Fig. 3) indicates that, as expected, the bands below −12.8 eV are the tin s states while the valence band, between −5.12 and −11.2 eV, is predominantly tin p states. In order to evaluate further the bonding in this compound, we calculated crystal orbital overlap population (COOP) curves for the different Sn–Sn interactions (Fig. 4). They showed that the main bonding states occur within the largest peak of the valence band in the DOS, between −11 and −8 eV, while the states of the same band above −8 eV are predominantly nonbonding, i.e. lone-pair like, as should be. The states above the Fermi level are clearly antibonding for all interactions around Sn3 (Fig. 4b–d) while for the Sn2–Sn2 interactions they remain nonbonding. The lowest-lying antibonding states are for the longest bond in the structure, 3.108(1) Å for Sn3–Sn3 (Fig. 4d).

4. Conclusions

A new ternary Zintl phase, $Ba_3Li_4Sn_8$, has been synthesized and structurally characterized. Its structure consists of chains made of edge-sharing cyclodecane-like units of tin in their 'all-chair' conformations. The Li^+ and Ba^{2+} cations screen the chains from each other and provide the extra electrons needed for chemical bonding and the compound is electronically balanced. However, the compound shows temperature-independent paramagnetism,

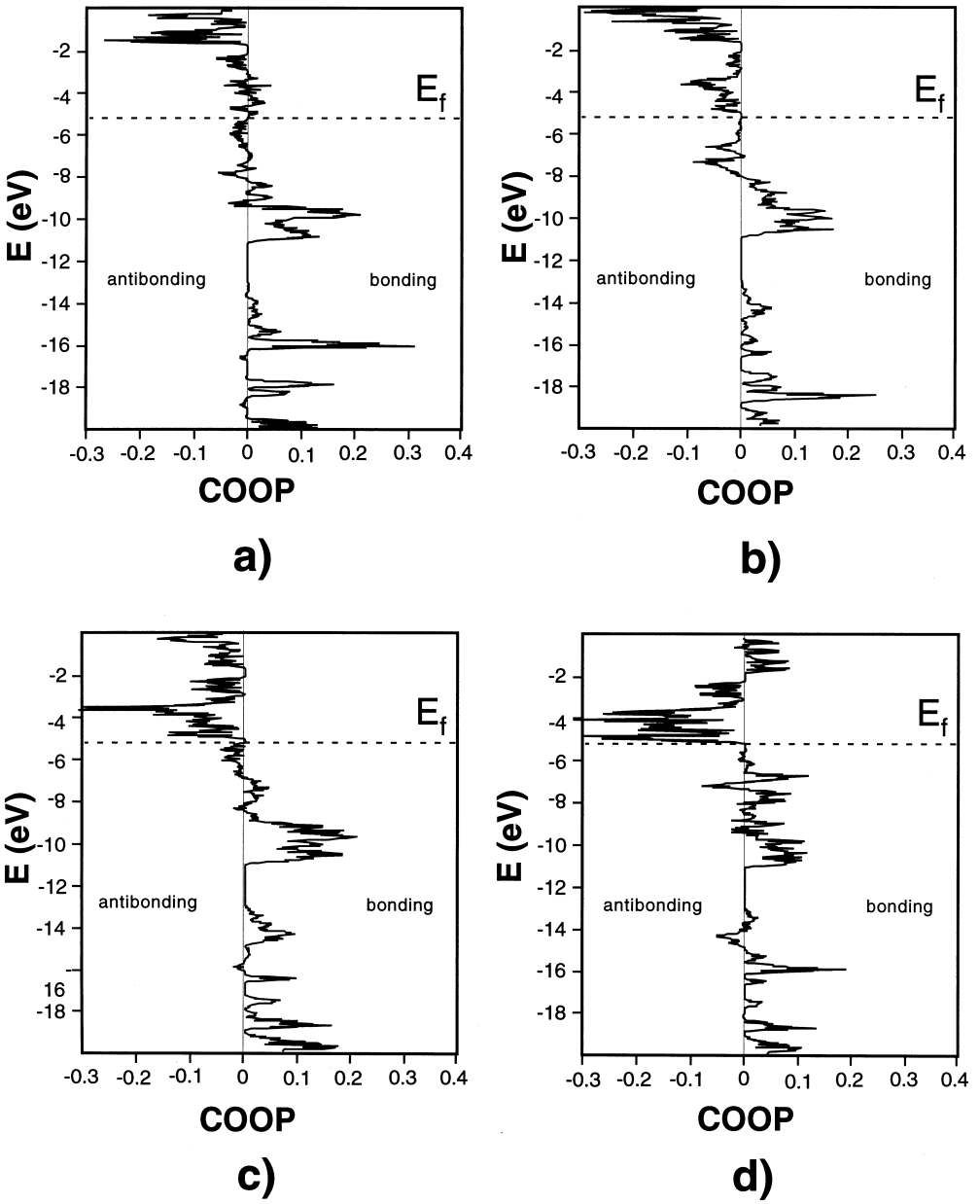

Fig. 4. COOP curves for the four different Sn–Sn bonds in $Ba_3Li_4Sn_8$: (a) Sn2–Sn2; (b) Sn1–Sn3; (c) Sn2–Sn3; (d) Sn3–Sn3.

which is most likely due to either van Vleck paramagnetism due to a very small band gap of 0.3 eV, or because of actual overlap of the conduction and valence bands.

Acknowledgements

We thank the Petroleum Research Fund, administered by the ACS, for the financial support of this research.

References

[1] V. Quenéau, S.C. Sevov, Angew. Chem. Int. Ed. Engl. 36 (1997) 1754.
[2] V. Quenéau, E. Todorov, S.C. Sevov, J. Am. Chem. Soc. 120 (1998) 3263.
[3] V. Quenéau, S.C. Sevov, Inorg. Chem. 37 (1998) 1358.
[4] E. Todorov, S.C. Sevov, Inorg. Chem. 37 (1998) 3889.
[5] J.D. Corbett, Chem. Rev. 85 (1985) 383.
[6] J.D. Corbett, Angew. Chem. Int. Ed. 39 (2000) 670.
[7] S. Bobev, S.C. Sevov, Angew. Chem. Int. Ed. 39 (2000) 4108.
[8] S. Bobev, S.C. Sevov, Angew. Chem. Int. Ed. 40 (2001) 1507.
[9] S. Bobev, S.C. Sevov, Polyhedron (2002) in press (published on the Web on January 13, 2002).
[10] S. Bobev, S.C. Sevov, Inorg. Chem. 40 (2001) 5361.
[11] S. Bobev, S.C. Sevov, J. Am. Chem. Soc. (2002) in press.
[12] S. Bobev, S.C. Sevov, Inorg. Chem. 38 (1999) 2672.
[13] Bruker Analytical Systems, Madison, WI, 1997.
[14] R.J. Hoffmann, J. Chem. Phys. 39 (1963) 1397.
[15] W. Müller, H. Schäfer, A. Weiss, Z. Naturforsch. 25b (1970) 1371.
[16] T.F. Fässler, S. Hoffmann, Z. Kristallogr. 214 (1999) 722.
[17] A.K. Ganguli, A.M. Guloy, E.A. Leon-Escamilla, J.D. Corbett, Inorg. Chem. 32 (1993) 4349.
[18] T.F. Fässler, C. Kronseder, Angew. Chem. Int. Ed. Engl. 36 (1997) 2683.
[19] R. Nesper, Prog. Solid State Chem. 20 (1990) 1.